Appl. Phys. B 70 [Suppl.], S193–S196 (2000) / Digital Object Identifier (DOI) 10.1007/s003400000364

Applied Physics B
Lasers
and Optics

Control of thermal effects for high-intensity Ti:sapphire laser chains

M. Zavelani-Rossi*, F. Lindner, C. Le Blanc, G. Chériaux, J.P. Chambaret

Laboratoire d'Optique Appliquée, ENSTA-Ecole Polytechnique-CNRS UMR 7639, Batterie de l'Yvette, 91761 Palaiseau cedex, France

Received: 1 October 1999/Revised version: 20 March 2000/Published online: 24 May 2000 –

Abstract. We have experimentally studied thermal effects in highly pumped Ti:sapphire crystals in the 140–340 K temperature range. We demonstrate that a critical temperature exists, which depends on pumping and probing conditions, below which detrimental thermal effects completely disappear. In particular, we show that in a typical high-intensity Ti:sapphire amplifier, thermal lensing and wave-front distortions can be suppressed keeping the crystal temperature lower than ~ 230 K.

PACS: 42.60.Da; 42.60.Jf; 65.90.+i

There is a growing interest in the generation of high-peak power ultrashort laser pulses for several applications both developed and proposed, such as high-order harmonic and X-ray generation [1–4]. These pulses are generated by laser systems based on the chirped pulse amplification (CPA) and are usually composed of different amplification stages to achieve the desired energy. In laser amplifiers the gain medium rods are pumped by high average power lasers; as a consequence the heat load is important and thermal effects in the rods are not negligible [5–10]. The amplified pulses can then be affected by thermal lensing, higher-order aberrations, and thermally induced distortions. The thermal lensing is particularly dangerous because it causes a reduction in the amplified mode spot size, eventually resulting in optical damages. Even if it can be compensated for, to some extent, by corrective optics such as diverging lenses, aberrations and distortions in the wave front are difficult to correct. To avoid all undesired effects it is thus necessary to control all detrimental thermally induced phenomena.

The most common and widely used approach is to predict the thermal effects and to exploit or compensate for them, when it is possible. Different numerical and analytical models have been developed to calculate the temperature distribution in the pumped rod [5, 9–15], the thermal lens and its aberrations [5, 7–11, 14–19], and other thermal effects such as thermal stress or birefringence [10, 15]. These models show that thermal lensing increases with the average pump intensity and with the variation of the medium index of refraction (n) with temperature (T) ($\partial n/\partial T$) and decreases with the thermal conductivity of the medium, although it cannot be correctly described by a simple induced lens. In high repetition rate systems (~ 1 kHz), a method to exploit thermal effects has been recently demonstrated [20]. It uses the pump-induced thermal lens to transform a classic multipass amplifier into a real eingenmode cavity. In this system lensing effects are properly controlled but distortions and higher-order aberrations can be still present [7–11, 15–19]. This method can be applied only in the high average pump intensity regime ($1–2$ kW/cm^2), typical of kHz systems, where thermal lensing is particularly strong [20].

A different approach is to find the conditions that permit limiting or even suppressing thermal effects. In the case of YAG crystals, Brown [19] proposed cooling the rods down to 77 K. Shulz and Henion [7] proposed the same for Ti:sapphire. Actually the thermal conductivity of the sapphire crystal dramatically increases upon decreasing the temperature [21] and its ($\partial n/\partial T$) decreases upon decreasing the temperature [22]. The cryogenic solution presents several advantages. First of all, by this method it could be possible to suppress not only thermal lensing but also higher-order aberrations and distortions. It allows the avoidance of the introduction of corrective optics which can add aberrations on the amplified beams. Moreover, it can be applied to any amplifier laser chain, independently of its repetition rate. Finally, the cooling solution enables simplification of the amplifier design and makes its alignment easier and independent of the pump power. It has been shown [7] that cooling the Ti:Al_2O_3 crystal of a single-transverse-mode laser down to 93 K improved the output power by more than two orders of magnitude with respect to the room temperature condition. Very recently a 0.2-TW laser system at 1 kHz has also been developed in which thermal lensing has also been eliminated by cooling the Ti:sapphire crystal down to 125 K [23, 24].

In this work we report on an experimental study of thermal effects in Ti:sapphire crystals in the 140–340 K temperature range. Our final aim is to verify the possibility of com-

*Corresponding author.
(Fax: +33-1/6931-9996, E-mail: zavelani@enstay.ensta.fr)

pletely cancelling detrimental thermal phenomena in high-intensity laser amplifiers. We pumped a Ti:sapphire crystal and probed the thermal pumping effects with a He-Ne laser beam. We varied the rod temperature and we measured spatial and phase profile under various pump, probe, and cooling conditions. We considered the steady-state equilibrium situation, neglecting transient phenomena which are not relevant to our present purpose. We first show that the thermal lens can be completely suppressed keeping the rod temperature lower than a critical value, which depends not only on the pump average intensity, but also on the pump and probe geometry. We then considered wave-front distortions due to thermal effects and we show that they disappear for rod temperatures lower than ~ 270 K. Finally, we experimentally compared a 1-kHz multipass amplifier water cooled with the same cryogenically cooled. We found that better performances could be achieved in the second case.

We performed the experiments using a 15×15-mm-large, 1-cm-long Ti:sapphire crystal, mounted in a copper heat sink in thermal contact with a commercial cryogenic cooler, and placed in a vacuum chamber. The temperature could be continuously varied from 140 to 340 K. In a first set of measurements we pumped the crystal with two collinear counter-propagating top-hat beams generated by a duplicated 100-Hz Q-switched Nd:YAG laser, with a total average intensity up to 220 W/cm^2, on a 1.3-mm spot size (for a 2.2-J/cm^2 fluence). This is the pumping condition of the first amplifier stage of a CPA system. We used, as a probe, a cw He-Ne laser beam passing through the crystal. We kept the angle between the pump and the probe as small as possible, as it is usual in multipass amplifiers for the pump and the amplifying beams. The beam produced by the He-Ne laser passed through a filtering system and a telescope; we changed the lens and adjusted the telescope to make the He-Ne beam almost collimated with the spot size inside the rod smaller or greater than the pump beam one, namely, 0.47, 0.88, 1.50, and 1.83 times the pump spot size. We then detected the beam at the output of the rod: the intensity profile with a CCD-array camera and the wave front and its distortions with a 2D Shack–Hartmann analyser, placed at a distance of ~ 1 m from the crystal.

We first measured the beam spot size variations as a function of temperature at a pump intensity of 220 W/cm^2. In Fig. 1 we show the result for probe beams smaller (diamonds) and larger (circle) than the pump beam. We plot also, as dashed lines, the spot sizes measured when the crystal was not pumped. From the figure it is evident that at low temperatures (around ~ 200 K) the He-Ne spot size measured with and without the pump beam action are the same. This is an indication that thermal lens effects are completely negligible. Increasing the rod temperature thermal lens becomes effective, inducing a reduction of the probe spot size, from a certain temperature forward, even if a thermal lensing effect which continuously increases with temperature was to be expected [5, 7–11, 14–19]. Moreover it is important to note that there are two critical temperatures at which a thermal lens begins to affect the probe beam. These values depend on the ratio between the probe spot size (w_{probe}) and the pump one (w_{pump}), $R = w_{\text{probe}}/w_{\text{pump}}$. In particular, whenever $R < 1$ the measured critical temperature is 260 K, while whenever $R > 1$ this temperature is 230 K, independently from the particular probe spot size. The reason for the lower critical value for $R > 1$ can be ascribed to an enhanced lensing effect due to the fact that the pump beam profile is not top-hat all over the probe beam [9, 14, 18]. We came to the same conclusions from the measure of the probe radius of curvature. The value of the critical temperature also depends on the pump average intensity. As a matter of fact, at a pump average intensity of 110 W/cm^2 we measured a critical temperature of 280 K using a probe beam with $R < 1$, as shown in Fig. 2.

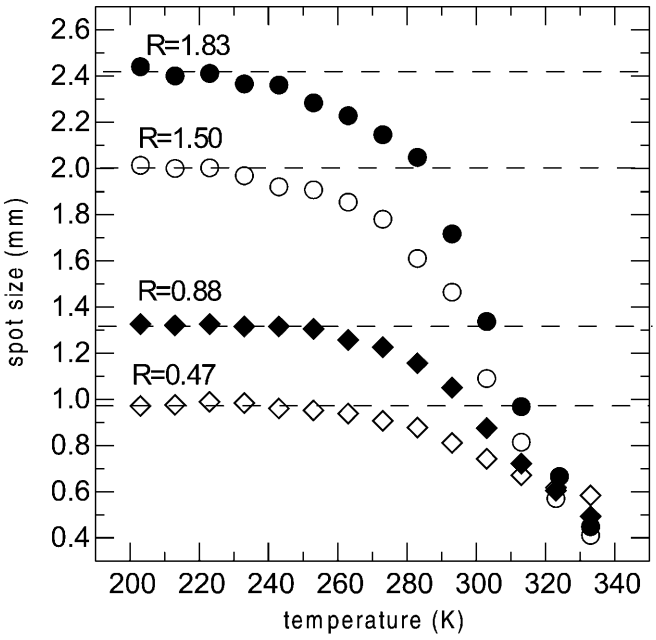

Fig. 1. Detected He-Ne spot size vs. temperature for different ratios between the probe and pump spot sizes inside the crystal ($R = w_{\text{probe}}/w_{\text{pump}}$, w being the spot size); *empty diamonds* correspond to $R = 0.47$, *filled diamonds* to $R = 0.88$, *empty circle* to $R = 1.50$ and *filled circle* to $R = 1.83$. The pump beam was top-hat at an average intensity of 220 W/cm^2. The *dashed lines* represent the spot size values of the He-Ne beams detected when the Ti:sapphire crystal was not pumped

We performed a second set of experiments in order to measure the wave-front distortions due to thermal effects, keeping the pump intensity constant at its maximum value. We detected the wave-front variations for beams with $R = 0.88$ and $R = 1.5$. Figure 3 shows the peak-to-valley (PV) and the root-mean-square (rms) values for the greater (filled and empty circle, respectively) and for the smaller (filled and empty diamonds) probe beam. At low temperatures (around 200–250 K) the probe mean distortions measured with and without (dashed lines in Fig. 3) the pump beams are the same. Thermally induced distortions in the pumped case begin to appear at a temperature $T \approx 290$ K for a probe beam with $R < 1$ and $T \approx 270$ K for $R > 1$. It is very interesting to note that wave-front distortions due to thermal effects do not affect the beams passing through a pumped region when the crystal temperature is kept low enough. Moreover, the experimental data show that when a Ti:sapphire rod is cooled down to a temperature for which the thermal lens is ineffective, then even the thermal distortions are completely suppressed.

In order to verify and to complete our previous results, we made the possible thermal effects stronger by pumping the crystal with an intensity of 5.2 kW/cm^2 using a cw argon laser beam focalised on a 200-μm-large spot. Indeed the Gaussian pump beam profile causes stronger thermal lensing

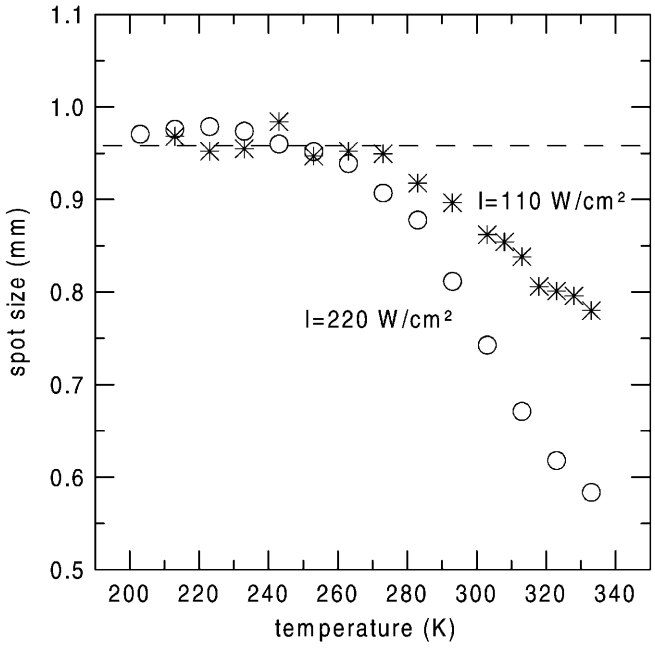

Fig. 2. Detected He-Ne spot size vs. temperature for different average pump intensity (I): *circle* for a pump intensity of 220 W/cm^2 and *stars* for 110 W/cm^2. R was 0.47. The pump beam was top-hat with a 1.3-mm spot size. The *dashed line* represents the spot size value of the He-Ne beam detected when the Ti:sapphire crystal was not pumped

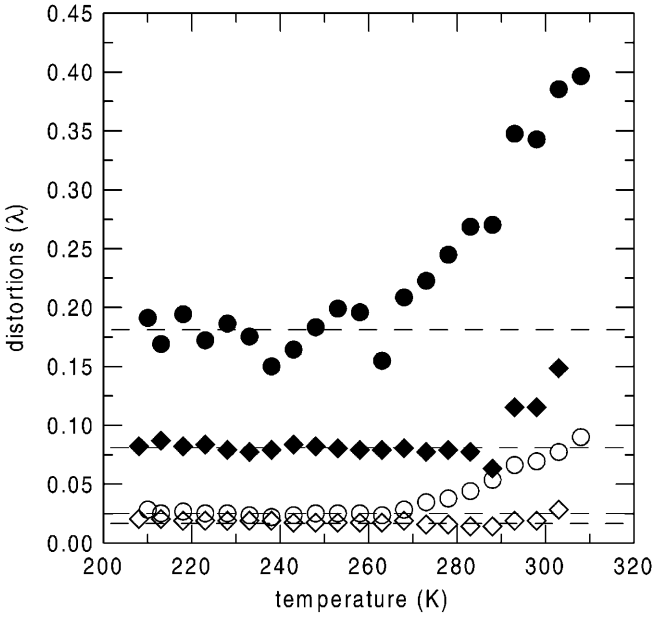

Fig. 3. Detected wave-front distortions of the He-Ne beam vs. temperature, PV (*filled symbols*) and rms (*empty symbols*) values, for the probe spot size larger (*circle*) and smaller (*diamonds*) than the pump spot size ($R = 1.5$ and $R = 0.88$, respectively). The pump beam was top-hat at an average intensity of 220 W/cm^2. The *dashed lines* represent the mean distortions of the He-Ne beams detected when the Ti:sapphire crystal was not pumped

than the top-hat one [9, 14, 18]. We probed thermal phenomena by means of a He-Ne beam with a 500-μm spot size and a 1-m radius of curvature at the rod. In this case the pump and the probe are collinear, to ensure a better superposition of the two beams, and the rod is pumped from only one end. The CCD-array camera and Shack–Hartmann wave analyser are placed 2.4 m from the crystal.

Figure 4 shows the He-Ne spot size measured by the CCD-array camera for different temperatures, for the pumped and nonpumped case. The experimental data show that for values of the temperature lower than 155 K the beam profile is not affected by lensing effects. We had the same result measuring the wave-front radius of curvature with the Shack-Harman analyser. As a matter of fact, it comes out that even in these strong conditions it is possible to completely cancel the thermal lens.

We then considered the beam wave-front distortions as a function of temperature. Figure 5 shows the measured PV and rms values for the pumped and nonpumped case. We note that for temperatures higher than ~ 275 K the beam greatly suffers distortions. In contrast, at lower temperatures it is not possible to identify distortions which could be ascribed to thermal effects. We thus note again that a Ti:sapphire crystal cooled down to a temperature for which the thermal lens effect is cancelled, does not introduce distortions in beams which pass through it. Besides, bearing this and the previous results in mind, it appears that, in general, to suppress thermally induced distortions it is only necessary to cool the Ti:sapphire crystals to temperatures lower than ~ 270 K.

As a further result, we observed that at temperatures higher than ~ 190 K some rings, due to thermal phenomena [18], appear in the probe beam intensity profile. We could no longer notice them at lower temperatures.

Finally, we tested the cooling solution directly on a Ti:sapphire 1-kHz three-pass amplifier of a CPA system [25]. We studied the thermal effects and compared the performances of the standard configuration, with the laser crystal water cooled, and that of the new solution, with the rod cryogenic cooled, in terms of output energy, beam profile, and wave-

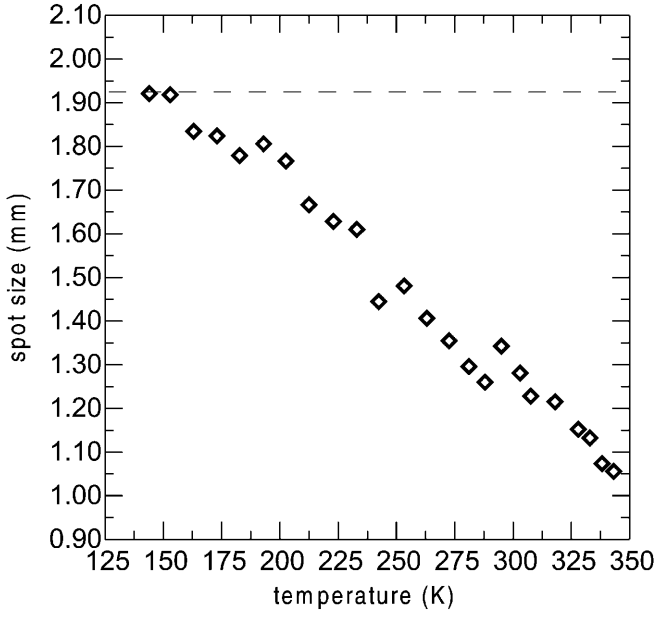

Fig. 4. Detected spot size vs. temperature of the He-Ne beam for a cw Gaussian pump beam. The pump intensity was 5.2 kW/cm^2 and its spot size on the crystal was 200-μm large; the probe spot size on the crystal was 500-μm large. The *dashed line* represents the spot size value of the He-Ne beam detected when the Ti:sapphire crystal was not pumped

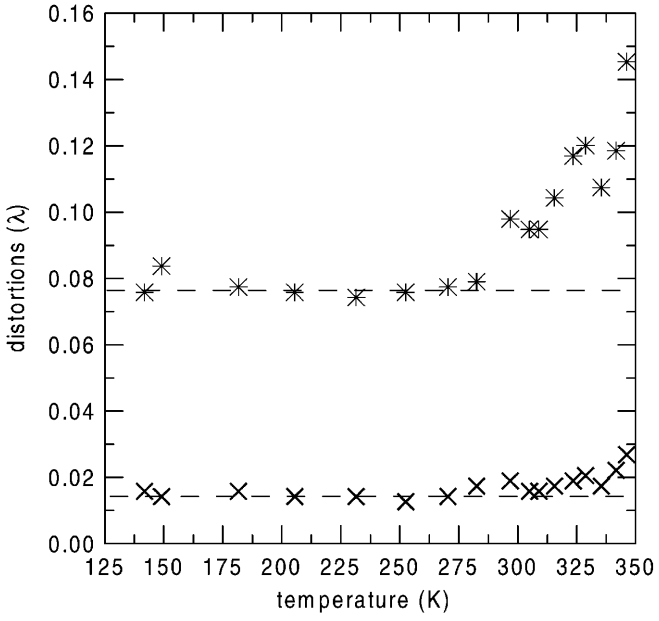

Fig. 5. Detected wave-front distortions of the He-Ne beam vs temperature, PV (*stars*) and rms (*cross*) values, for a cw Gaussian pump beam. The pump intensity was 5.2 kW/cm^2 and its spot size on the crystal was 200-μm large; the probe spot size on the crystal was 500-μm large. The *dashed lines* represent the mean distortions of the He-Ne beam detected when the Ti:sapphire crystal was not pumped

front distortions. The crystal was pumped at a total average intensity of 1.75 kW/cm^2 (1.75-J/cm^2 fluence), on a spot size of 750 μm, by two counter-propagating beams of two Q-switched duplicated Nd:YLF lasers. It was then traversed by a pulsed beam at 800 nm which was amplified at each passage. Its spot size in the crystal was nearly the same of that of the pump beam. In the water-cooled case the rod temperature was 300 K, while with the cryogenic cooler it was 200 K.

We first analysed the thermal lens induced by the pump on the infrared beam after its first pass, using the Shack–Hartmann detector. We measured a thermal lensing effect almost three times lower at 200 K with respect to the one at 300 K. It is worth mentioning the fact that in the water-cooled condition we were obliged to insert two diverging lenses, in the three-pass path of the infrared beam, to compensate for the thermal lens. In the case of cryogenic cooling, there was no need to insert any corrective optics.

The output energy was the same in the two cases ($\sim$ 10 mJ), but it is very important to note that in the case of water cooling the output beam presented a ring pattern profile which was completely absent using the cryogenic cooling. In this second case we obtained a uniform beam profile with a Strehl ratio of 0.99 [26].

Finally, we analysed the thermal wave-front distortions. Actually we could not notice any significant difference between the two different conditions. We measured PV values of the order of $\lambda/10$ and rms values of $\lambda/60$, which means that higher-order thermal effects were negligible. This result is consistent with the previous ones on distortions; in fact, in the cryogenic-cooled condition the rod temperature was lower than 270 K so we did not expect any thermally induced distortions; in the water-cooled condition we expected only small distortions being the rod temperature near, even than higher, to 270 K.

In conclusion, we have experimentally studied thermal effects in highly pumped Ti:sapphire crystals in the temperature range 140–340 K. We found that in any pumping and probing situation a critical temperature exists below which detrimental thermal effects completely disappear. In particular, we showed, for the first time to our knowledge, that in typical high-intensity Ti:sapphire amplifiers, thermal lensing and wave-front distortions can be suppressed by keeping the crystal temperature lower than $\sim$ 230 K.

References

1. A. Huillier, P. Balcou: Phys. Rev. Lett. **70**, 774 (1993)
2. J.J. Macklin, J.D. Kmetec, C.L. Gordon III: Phys. Rev. Lett. **70**, 766 (1993)
3. J. Zhou, J. Peatross, M.M. Murnane, H.C. Kapteyn, I.P. Christov: Phys. Rev. Lett. **76**, 752 (1996)
4. Z. Chang, A. Rundquist, H. Wang, H.C. Kapteyn, M.M. Murnane: Phys. Rev. Lett. **79**, 2967 (1997)
5. W. Koechner: *Solid State Laser Engeneering* (Springer Series in Optical Sciences, Springer, Berlin, Heidelberg 1996)
6. S. De Silvestri, P. Laporta, V. Magni: IEEE J. Quantum Electron. **QE-23**, 1999 (1987)
7. P.A. Schulz, S.R. Henion: IEEE J. Quantum Electron. **QE-27**, 1039 (1991)
8. M.D. Skeldon, R.B. Saager, W. Seka: IEEE J. Quantum Electron. **QE-19**, 381 (1999)
9. J. Frauchiger, P. Albers, H.P. Weber: IEEE J. Quantum Electron. **QE-28**, 1046 (1992)
10. C. Pfistener, R. Weber, H.P. Weber, S. Marazzi, R. Gruber: IEEE J. Quantum Electron. **QE-30**, 1605 (1994)
11. S.J. Sheldon, L.V. Knight, J.M. Thorne: Appl. Opt. **21**, 1663 (1982)
12. U.O. Farrukh, A.M. Buoncristiani, C.E. Byvik: IEEE J. Quantum Electron. **QE-24**, 2253 (1988)
13. U.O. Farrukh, P. Brockman: Appl. Opt. **32**, 2075 (1993)
14. M.E. Innocenzi, H.T. Yura, C.L. Fincher, R.A. Fields: Appl. Phys. Lett. **56**, 1831 (1990)
15. A.K. Cousins: IEEE J. Quantum Electron. **QE-28**, 1057 (1992)
16. C.A. Carter, J.M. Harris: Appl. Opt. **23**, 476 (1984)
17. J. Shen, R.D. Lowe, R.D. Snook: Chem. Phys. **165**, 385 (1992)
18. F. Jürgesen, W. Schröer: Appl. Opt. **34**, 41 (1995)
19. D.C. Brown: IEEE J. Quantum Electron. **QE-34**, 2383 (1998)
20. F. Salin, C. Le Blanc, J. Squier, C. Barty: Opt. Lett. **23**, 718 (1998)
21. M.G. Holland: J. Appl. Phys. **33**, 2910 (1962)
22. A.C. De Franzo, B.G. Pazol: Appl. Opt. **32**, 2224 (1993)
23. S. Backus, C.G. Durfee III, G. Mourou, H.C. Kapteyn, M. Murnane: Opt. Lett. **22**, 1256 (1997)
24. C.G. Durfee III, S. Backus, M.M. Murnane, H.C. Kapteyn: IEEE J. Sel. Top. Quantum Electron. **4**, 395 (1998)
25. C. Le Blanc, E. Baubeau, F. Salin, J.A. Squier, C.P.J. Barty, C. Spielmann: IEEE J. Sel. Top. Quantum Electron. **4**, 407 (1998)
26. S. Ranc, G. Chériaux, S. Ferré, J.P. Rousseau, J.P. Chambaret: in the same journal